Fuel Processing Technology, Volume 195, 1 December 2019, Article number 106143
DOI:10.1016/j.fuproc.2019.106143

Sorption of CO_2 on NaBr co-doped Li_4SiO_4 ceramics: Structural and kinetic analysis

Ke Wang[1,2], Youwei Zhao[1], Peter T. Clough[2], Pengfei Zhao[1], Edward J. Anthony[2*]

[1] School of Electrical and Power Engineering, China University of Mining and Technology, Xuzhou 221116, China.

[2] Energy and Power Theme, Cranfield University, Cranfield, Bedfordshire, MK43 0AL, UK.

Ke Wang is currently a visiting professor at Cranfield University.

* Corresponding author: Edward J. Anthony, E: b.j.anthony@cranfield.ac.uk,

T: +44 (0) 1234 752 823

Abstract: Structurally modified and improved NaBr co-doped Li_4SiO_4 ceramics were developed for CO_2 absorption in low-CO_2-concentration atmospheres. Pure and NaCl-doped Li_4SiO_4 ceramics were also prepared for comparison. The samples were analyzed by X-ray diffraction, Scanning Electron Microscopy, N_2 adsorption, X-ray photoelectron spectroscopy, differential scanning calorimetry, and thermogravimetric analyses (dynamic and isothermal). The sorption kinetics were obtained using a double exponential model. The results showed that both Na and Br can be introduced into the Li_4SiO_4 structure and doped on Li and oxygen sites, respectively. The doped sample presented a Li_2O-enriched surface, guaranteeing abundant Li-O sites and our significantly different from previous anionic (CO_3, F and Cl) doping of Li_4SiO_4, Br doping also generated macroporous features with small particle size. These favorable characteristics promoted the surface chemisorption kinetics. Moreover, DSC analysis confirmed the formation of the molten phases during CO_2 absorption, which helps improve the lithium diffusion kinetics. Here, 0.1 mol NaBr doping was used to reach a maximum absorption capacity (>30.0 wt.%) in 15 vol.% CO_2, suggesting that NaBr-doped Li_4SiO_4 ceramics have great potential for CO_2 capture at high temperature.

Keywords: CO_2 capture; NaBr doping; carbon template; Li_4SiO_4

Highlights

Ceramics of NaBr co-doped Li4SiO4 were synthesized for the first time.

Small-sized Li4SiO4 grains with macro porous features were obtained.

Li-O rich sites were found on the surface during CO_2 sorption.

These desirable features resulted in superior CO_2 capture performance.

1. Introduction

Rising anthropogenic CO_2 emissions are causing climate change [1] and carbon capture and storage (CCS) is an effective way to continue using fossil fuels and still meet ambitious CO_2 emission targets [2]. However, current CCS technologies utilizing aqueous amines have large energy losses, mainly associated with the amine regeneration/CO_2 separation step [3]. To increase the useful energy of these system and decrease the operating costs, intermediate-temperature and high-temperature sorbents, including hydrotalcites [4], MgO-based sorbents [5], calcium oxides [6-9], and ceramic materials [10-12], have been examined as alternative sorbents because these materials can directly separate CO_2 from hot flue gases in thermal power or sorption-enhanced steam methane reforming (SE-SMR) processes. Alkaline ceramic materials [13], especially lithium orthosilicate (Li_4SiO_4) [14, 15], appear to be attractive sorbents because they have high theoretical CO_2 capture capacities (36.7 wt.%), and a consistent recyclability.

Solid-state Li_4SiO_4 fabricated by traditional methods has an extremely low porosity and typically very large particle/grain size, making the reaction between Li_4SiO_4 and CO_2 relatively slow [16]. To decrease particle sizes and increase its specific surface area, several synthetic routes, including ball milling [17, 18], impregnated suspension [19-21], precipitation [22], sol–gel techniques [23-25], carbon templates or porous carbon [26-28] and hydration [29], have been suggested. Unfortunately, these

morphologically-improved particles still exhibited unsatisfactory reaction kinetics (~10^{-4} s^{-1}) under typical hot flue gases in thermal power applications or under SE-SMR conditions [29, 30].

To further improve the kinetics under low CO_2 partial pressure conditions, doping of foreign materials [31, 32], especially alkali carbonates [33, 34], into Li_4SiO_4 particles has been studied. Zhang et al. [35] and Seggiani et al. [36] prepared K_2CO_3- or Na_2CO_3-doped Li_4SiO_4 particles by means of a solid-state reaction. Yang et al. [37] designed alkali carbonate-doped sorbents with micron-sized pores using an impregnated suspension method. Xiang et al. [38] synthesized a relatively porous Na and Ti co-doped sorbent using a sol–gel method. Subha et al. [39] fabricated a nanorod (Li−Na−K)CO_3-coated Li_4SiO_4 material by a microwave sol–gel process. Recently, Wang et al. [40, 41] developed a novel anionic (F or Cl) doping technique to modify the intrinsic properties of Li_4SiO_4 through a sacrificial carbon template and hydration techniques. Both NaF- and NaCl-doped Li_4SiO_4 showed superior CO_2 absorption performance. It appears that in the high-temperature absorption process, anionic (CO_3, F and Cl) doping forming low-temperature eutectic compounds which significantly reduced the diffusion resistance of CO_2 [29, 40, 42]. However, the anionic doping also suffered from serious sintering problems, inducing severe grain aggregation and porosity loss, which resulted in poorer kinetic performance.

Unlike previous anionic (CO_3, F and Cl) doping, this work used NaBr for the first time as a new dopant to tailor Li_4SiO_4 ceramic materials with different macroporous morphologies. Based on the structure, morphology and kinetic characteristics, the impacts of NaBr doping on the CO_2 chemisorption properties of Li_4SiO_4 were explored.

2. Experimental

2.1 Sorbents

All chemicals used were analytical grade (from Aladdin Chemical Reagent Co., Ltd.). To obtain the Na-doped samples, pure Li_4SiO_4 and Na sources (NaCl and NaBr)

were selected. In the preparation process of pure Li_4SiO_4, fumed silica and lithium nitrate were weighed accurately to a mole ratio of 4.1:1 of $LiNO_3$:SiO_2, and after blending together the mixture was calcined at 800 °C for 4 h. An excess of 0.1 mols lithium was added to reduce the problems caused by the sublimation of lithium at high temperatures. The powder synthesized in the high-temperature solid-state reaction was designated PS.

The Na-doped samples were formed by the sacrificial carbon template method (SCT) via the gluconic acid pyrolysis process. This procedure involved incorporating a certain amount of Na dopant, PS sample and gluconic acid in an aqueous solution. These reagents were mixed according to a molar ratio of X:1:2 of Na:Li_4SiO_4:gluconic acid, where X=0.1, 0.04 or 0.5. The resulting solution was constantly stirred at 80 °C until a wet gel was formed. After drying at 105 °C for 24 h, the obtained powder was calcined at 500 °C in pure N_2 in a muffle furnace to ensure sufficient pyrolysis and then further preheated at 700 °C for 4 h in air. The final samples obtained were designated as SCT-NaBr-0.1, SCT-NaCl-0.1, SCT-NaBr-0.04, SCT-NaCl-0.04, SCT-NaBr-0.5 and SCT-NaBr-0.5 based on the dopant type and quantity used. A control sample without Na doping was made using the same sacrificial carbon template method and designated as SCT [26].

2.2 Characterization

The crystal phases of the samples were analyzed by a Bruker Model D8 Advance X-ray diffractometer (XRD) in the 2θ range of 10-70°. A Hitachi Model S-4800 scanning electron microscope (SEM) was used to record the morphologies of the prepared samples. The pore properties, including the specific surface area, pore volume and size distribution were measured using a Quantachrome Novawin N_2 adsorption/desorption analyzer. X-ray photoelectron spectroscopy (XPS) spectra were obtained using a Perkin-Elmer PHI 5600 XPS to analyze the surface atomic concentrations and bonding, the data from which were processed using the

XPSPEAK41 software packages. The differential scanning calorimetry (DSC) data were obtained with a Labsys Evo along with data from a simultaneous thermal thermogravimetric analyzer under a pure CO_2 atmosphere, covering a temperature range from room temperature to 1000 °C, with a heating rate of 5 °C/min for a flow rate of 0.05 dm^3/min.

2.3 CO_2 sorption

The CO_2 absorption was measured using a thermogravimetric analyzer (ZRY-1P, Techcomp Jingke Scientific Instrument Co., Ltd., Shanghai, China). The samples were weighed, placed in an alumina crucible, and heated from room temperature to 1000 °C at a heating rate of 10 °C/min under a 15 vol.% CO_2 atmosphere (balance with N_2) Isothermal experiments were carried out at 475 °C, 525 °C and 575 °C for 120 min under a 15 vol.% CO_2 atmosphere balanced with N_2 using a total flow rate of 0.05 dm^3/min.

3. Results and discussion

3.1 Characterization

The crystal phases, surface composition, grain morphologies and porous properties of the prepared samples were examined by XRD, XPS, SEM and nitrogen absorption. The XRD patterns (Fig. 1a) showed the pure diffraction peaks of Li_4SiO_4 with a monoclinic structure. At low dopant concentrations of NaCl of 0.04 (molar ratio Na relative to Li_4SiO_4), no secondary phases (such as Li_2SiO_3) were detected in the pattern for SCT-NaCl-0.04, which suggests that all the NaCl was incorporated into the Li_4SiO_4 lattice to produce a solid solution. When the amount of dopant was increased to 0.1, the diffraction peaks of NaCl were identified in SCT-NaCl-0.1, showing that the doping amount had exceeded the solubility limit within the Li_4SiO_4 structure. However, faint diffraction peaks of NaBr were identified in SCT-NaBr-0.04, and stronger diffraction peaks of NaBr were also detected in SCT-NaBr-0.1 showing that the Na was

not fully dispersed within the lattice. As reported for Cl-doped Li_2FeSiO_4 [43], both halogen ions (bromide and chloride) tended to be incorporated into the orthosilicate. On the other hand, the solubility limit of SCT-NaBr (<0.04) was lower than that of SCT-NaCl (>0.04) mainly due to the larger ionic radii of Br^- compared to that of Cl^-.

To examine shifts in the peak positions in detail, the peak in 2θ range of 21.8-23.0 for SCT, SCT-NaCl-0.04, and SCT-NaBr-0.04 are shown in Figure 1b. Doping with NaCl and NaBr caused the peak positions of the SCT sample to shift slightly toward a lower angle, suggesting a change in the crystal lattice of Li_4SiO_4. Based on Bragg's law, the lowering of 2θ generates an increased interplanar spacing, which can explain the increased lattice parameters as NaCl/NaBr is introduced into the Li_4SiO_4.

To further explore the NaCl/NaBr doping effect on the surface composition of Li_4SiO_4, XPS analysis was performed. As shown in Fig. 2a, the Li 1s spectra of SCT exhibited a peak at 54.0 eV, which is related to the presence of a Li_xSiO_y phase. For the two Na-doped samples, the peaks of both spectra shifted to a higher binding energy, suggesting that the introduced Na was doped on Li sites. This doping likely resulted in the generation of Li_2O at the surface due to the presence of Li_2O, which has a higher binding energy than Li_4SiO_4 [44]. The Si sites, Si 2p spectra are also identified in Fig. 2b. The binding energies recorded for SCT were ~100.7 eV, corresponding to the presence of a Li_4SiO_4 species [45]. After Na doping, a higher binding energy was observed for both NaCl/NaBr-doped samples mainly due to the formation of Na_2SiO_4 (102-104 eV) [46, 47].

Due to the absence of secondary phases observed in SCT-NaCl-0.04, the spectrum of Cl 2p is clearly displayed in Fig. 2c. There are two peaks (198.8 and 200.5 eV) in the spectrum of SCT-NaCl-0.04. Considering the effects of pure NaCl reported in previous work (198.4 and 200.0 eV) [48], the shifted spectrum of SCT-NaCl-0.04 most likely arises as a result of the Cl doping. Thus, the halogen ion doping on the O 1s spectrum is further shown in Fig. 2d. The O 1s peak at ~531.5 eV was observed in all three samples, which is attributed to the presence of Li_4SiO_4 [44]. For both halogen ion-

doped samples, there is another distinct shoulder near 528.4 eV that is assigned to the Li_2O species. Such significant changes in material environment confirm that the halogen ions were doped on oxygen sites, which agrees with the results of the Li 1s spectrum. The XPS analysis supported the XRD results, and further suggested that Na and halogen were introduced into the Li_4SiO_4 structure and doped on Li and oxygen sites. Moreover, based on peak-differentiating analysis, the amount of Li_2O determined for SCT-NaBr-0.1 (14.65%) is higher than that of SCT-NaCl-0.1 (9.56%), indicating Br doping induced the formation of more Li_2O-enriched Li_4SiO_4 than did Cl doping. Based on all these characterizations, Li_4SiO_4 doping with y mol of NaX can be described by equation 1 (X=Cl or Br):

$$y(NaX) + Li_4SiO_4 \rightarrow Li_{4-y}Na_ySiO_{(4-0.5y)}X_y + 0.5y(Li_2O) \quad (1)$$

The SEM images of three Li_4SiO_4 samples are illustrated in Fig. 3. The SCT showed macroporous particles (Fig. 3a). As shown in the high-magnification image (Fig. 3b), the co-existence of large and small sintered agglomerates was observed. Such morphologies are caused by the large amount of gas released during the high-temperature inhomogeneous decomposition. Upon NaCl doping, the morphologies of SCT-NaCl-0.1 were evidently even more sintered with larger and denser particles (Fig. 3c). Moreover, the macropores on the surface disappeared (Fig. 3d). In contrast to the NaCl doping, more macroporous morphologies were observed for NaBr doping. SCT-NaBr-0.1 also exhibited regular polyhedrons with smaller particles (Fig. 3e) and well interlinked macropores developed on the surface (Fig. 3f). It was reported that Br doped CaO also produce large macrospores [49]. These macroporous structures are incredibly useful for the transport of CO_2 to the interior of the agglomerates for CO_2 capture and release.

To specifically compare the porous structures of SCT-NaCl-0.1 and SCT-NaBr-0.1, isothermal N_2 adsorption/desorption measurements were characterized. The results are presented in Table 1. Three samples all presented low specific surface area and pore volume. However, the specific surface area and pore volume of SCT-NaBr-0.1 was

three times those of SCT-NaCl-0.1. The N_2 adsorption/desorption analyses support the SEM results, highlighting the more macroporous properties produced via the NaBr doping procedure.

Thermogravimetric analysis and differential scanning calorimetry (TGA/DSC) were conducted to determine the formation of molten phases during CO_2 absorption. To ensure that the endothermic behaviors are clearly observed, the doping quantity was increased from 0.1 to 0.5 here. The same procedure is also reported in the previous work [37]. As shown in Fig. 4, TGA results suggest that the undoped sample SCT started to trap CO_2 at ~530 °C and released CO_2 above 700 °C under an atmosphere of 100% CO_2. Accordingly, the DSC curves had a weak exothermic peak (~680 °C) suggesting that Li_4SiO_4 reacts exothermically with CO_2 at this temperature. There was also a strong endothermic peak (~720 °C) in the DSC curves, implying that the desorption process was endothermic. Similar exothermic/endothermic peaks are also reported in the former study [50]. Here, the TGA curves of two doped samples showed wider absorption/desorption temperature ranges. Their DSC curves thus displayed an exothermic peak at a lower temperature and an endothermic peak at a higher temperature. More importantly, another endothermic peak was observed for both doped sorbents between the exothermic peak and the endothermic peak, which must be related to the formation of the molten phases. The presence of molten compounds evidently significantly increased the lithium diffusion process [51].

3.2 CO_2 uptake characteristics and kinetic analysis

Figure 5a shows the dynamic curves for the three sorbents tested in an atmosphere of 15 vol.% CO_2. For reference, the SCT started to capture CO_2 at ~500 °C and desorbed CO_2 above 640 °C. Under this condition, only a 10.2wt.% increase occurred. A thick external layer [52] was formed and covered the surface of SCT. Thus, lithium diffusion resistance was greatly increased and a low CO_2 uptake was obtained for SCT. Upon doping, the initial absorption temperature in the SCT-NaCl-0.1 and SCT-NaBr-0.1

samples decreased. Similar results for other alkali carbonate-doped Li_4SiO_4 samples have also been previously reported [33]. Moreover, the two doped samples exhibited remarkably enhanced CO_2 absorption performance. SCT-NaBr-0.1 reached the highest absorption uptake (~29.1 wt.%), which was approximately 3 times as high as the maximum sorption for SCT. In addition, the absorption rates were greatly increased for the doped samples. Here, the slope of SCT-NaBr-0.1 (in the temperature range of 485-650 °C) was highest at 0.17 wt.% min^{-1}, showing nearly 3 times the absorption rate of the SCT (0.06 wt.% min^{-1}). Additionally, a slight weight loss was both obtained for two doped sample at higher temperature (> 800 °C). It seemed that such doped Li_4SiO_4 may experience an unexpected decomposition.

To further analyze the CO_2 capture process on these samples, isothermal experiments were conducted at 475 °C, 525 °C, and 575 °C for 2 h. At 475 °C, the SCT particles (Fig. 5b) showed extremely low capacities and absorption rates. When doped with NaCl or NaBr, the CO_2 capture amounts were enhanced, and the absorption rates were accelerated. In particular, SCT-NaBr-0.1 achieved the fastest absorption rate and the highest CO_2 capture ability. After the first 10 min of reaction with CO_2, the uptake of SCT-NaBr-0.1 exceeded 16.9%, which is 4 times as high as that of SCT. The absorption behaviors were similar but even more drastic affected for these three isotherms at 525 °C (Fig. 5c). However, SCT-NaBr-0.1 still demonstrated the fastest absorption rate and highest absorption capacity, and its absorption quickly saturated at 27.6 wt.% within 50 mins. In addition, the gap between SCT-NaBr-0.1 and SCT-NaCl-0.1 decreased compared with those at 475 °C. When the temperature was further increased to 575 °C, the superior CO_2 performance was retained for SCT-NaBr-0.1, as indicated in Fig. 5d. Interestingly, the maximum CO_2 capture capacity of SCT-NaCl-0.1 was slightly higher than that of SCT-NaBr-0.1. Similar results have also been seen for alkali nitrates-doped Li_4SiO_4 sorbents [53]. At higher temperature (575 °C), lithium diffusion resistance was greatly reduced. Thus, the improvements in the CO_2 capture process induced by sodium halides addition appeared to be independent of the halides

type.

These isothermal curves were fitted to double exponential models [21] to examine the absorption kinetics of three samples:

$$y=A\exp^{-k_1t}+B\exp^{-k_2t}+C \qquad (2)$$

in which y is the CO_2 absorption capacity; A, B and C represent the pre-exponential factors; t is the time; and k_1 and k_2 are exponential constants for the CO_2 chemisorption directly over the surface of Li_4SiO_4 particles and the CO_2 sorption kinetically controlled by lithium diffusion, respectively.

The values of the parameter obtained are listed in Table 2. All isothermal curves displayed good curve fits to double exponential models, indicating that the absorption process involved an initial surface chemisorption stage followed by a lithium diffusion stage. Moreover, the surface chemisorption constant values (k_1) were ten times as high as the lithium diffusion constant values (k_2), suggesting that lithium diffusion was the main limiting factor during the whole absorption process. Previous work [21, 52] suggested that as the absorption process progressed, the external layer formed (composed mainly of Li_2CO_3 and Li_2SiO_3) was thicker. Due to the absence of the molten layer (Fig. 4), the lithium diffusion resistance was greatly increased. Thus, slow absorption kinetics were shown for SCT. Furthermore, the k_1 and k_2 values of the doped sorbents were several times higher than those of SCT. As confirmed by DSC analysis, the molten phases formed for two co-doped sorbents promoted the lithium diffusion process very strongly, thereby improving the CO_2 absorption kinetics. More importantly, doping with different anions (Br and Cl) resulted in rather different absorption kinetics. In particular, the kinetics of the surface chemisorption were larger for SCT-NaBr-0.1 than for SCT-NaCl-0.1. The characterization results also show that Br doping induced more macroporous properties, smaller particle size and a more Li_2O-rich Li_4SiO_4 surface. In other words, a greater abundance of Li-O sites was formed [21], which gave rise to a higher surface chemisorption reactivity. However, at a high temperature of 575 °C, entirely different behavior was observed. The kinetics of the lithium diffusion

observed for SCT-NaCl-0.1 increased. It seemed that the lithium diffusion for SCT-NaBr-0.1 was smaller at higher temperatures.

To analyze the influence of temperature on the absorption kinetics, we used Eyring's model, which can be used for solid-gas reactions:

$$\ln (k/T) = (-\Delta H^{++}/ R)\ 1/T + \ln (k_B/h) + \Delta S^{++}/ R \quad (2)$$

where k is the reaction rate constant, T represents the absolute temperature, ΔH^{++} is the activation enthalpy, R represents the gas constant, k_B is the Boltzmann constant, h is Planck's constant and ΔS^{++} represents the activation entropy.

Fitting Eyring's model, the plots of ln (k/T) versus 1/T gave linear behavior as shown in Fig. 6 and the activation enthalpies were obtained from the slope. Compared with pure Li_4SiO_4 reported in previous studies [40, 54], the ΔH^{++} values of the surface chemisorption processes for SCT-NaCl-0.1 and SCT-NaBr-0.1 were greatly reduced, indicating the surface chemisorption process was less dependent on temperature when doping with NaCl/NaBr. Moreover, a decrease in the ΔH^{++} value of NaBr doping for surface chemisorption was observed as compared with the case of NaCl doping, indicating that its surface chemisorption was less reliant on temperature. For the lithium diffusion process, the $\Delta H^{++}$of SCT-NaBr-0.1 was also reduced. Both surface chemisorption and lithium diffusion on SCT-NaBr-0.1 doping were less dependent on temperature than for SCT-NaCl-0.1, mainly due to more favorable structure (more macroporous properties, smaller particle size and a more Li_2O-rich Li_4SiO_4 surface) upon NaBr doping.

4. Conclusions

Given that any lithium based material will be significantly more expensive than say a Ca based sorbent and the fact that there are many demands on the available supplies of Li, high recyclability and high absorption rates are critical for the development of Li based ceramic sorbents. Here, NaCl and NaBr co-doped Li_4SiO_4 sorbents were prepared via a sacrificial carbon template method. The doped sodium and

Cl/Br were incorporated into the Li_4SiO_4 structure and doped on Li and oxygen sites, respectively. The distinct anionic doping features induced significantly different grain morphologies, porous properties and surface compositions. Unlike Cl doping, Br doping induced the formation of smaller particle size, more macroporous properties and a more Li_2O-rich Li_4SiO_4 surface, ensuring abundant Li-O sites on the surface to facilitate chemisorption. At the same time, the molten phase formed when absorbing CO_2 greatly decreased the lithium diffusion resistance. Thus, a significantly faster absorption rate, higher CO_2 absorption capacity and greater absorption kinetics were obtained for SCT-NaBr-0.1 as compared with SCT.

Supplementary material

The dynamic DSC curves between 20 and 750 °C in a 100% CO_2 flux for three sorbents are presented (Fig. S1).

Acknowledgement

This work was supported by the Outstanding Teacher Overseas Research Project and the Fundamental Research Funds for Talents Cultivation Project of China University of Mining and Technology.

References

[1] S. Brune, S.E. Williams, R.D. Müller, Potential links between continental rifting, CO_2 degassing and climate change through time, Nat. Geosci., 10 (2017) 941-946.

[2] R.P. Cabral, N. Mac Dowell, A novel methodological approach for achieving pound/MWh cost reduction of CO_2 capture and storage (CCS) processes, Appl. Energy, 205 (2017) 529-539.

[3] F. Shakerian, K.H. Kim, J.E. Szulejko, J.W. Park, A comparative review between amines and ammonia as sorptive media for post-combustion CO_2 capture, Appl. Energy, 148 (2015) 10-22.

[4] X. Kou, C. Li, Y. Zhao, S. Wang, X. Ma, CO_2 sorbents derived from capsule-connected Ca-Al hydrotalcite-like via low-saturated coprecipitation, Fuel Process. Technol., 177 (2018) 210-218.

[5] W. Gao, T. Zhou, Y. Gao, B. Louis, D. O'Hare, Q. Wang, Molten salts-modified MgO-based adsorbents for intermediate-temperature CO_2 capture: A review, J. Ener. Chem., 26 (2017) 830-838.

[6] M. Benitez-Guerrero, J.M. Valverde, P.E. Sanchez-Jimenez, A. Perejon, L.A. Perez-Maqueda, Calcium-Looping performance of mechanically modified Al2O3-CaO composites for energy storage and CO_2 capture, Chem. Eng. J., 334 (2018) 2343-2355.

[7] Y. Hu, W. Liu, Y. Peng, Y. Yang, J. Sun, H. Chen, Z. Zhou, M. Xu, One-step synthesis of highly efficient CaO-based CO_2 sorbent pellets via gel-casting technique, Fuel Process. Technol., 160 (2017) 70-77.

[8] K. Wang, P.T. Clough, P. Zhao, E.J. Anthony, Synthesis of highly effective stabilized CaO sorbents via a sacrificial N-doped carbon nanosheet template, J. Mater. Chem. A, 7 (2019) 9173-9182.

[9] A. Coppola, A. Esposito, F. Montagnaro, M. Iuliano, F. Scala, P. Salatino, The combined effect of H_2O and SO_2 on CO_2 uptake and sorbent attrition during fluidised bed calcium looping, Proc. Combust. Inst., 37 (2019) 4379-4387.

[10] H. Pfeiffer, P. Bosch, Thermal Stability and High-Temperature Carbon Dioxide Sorption on Hexa-lithium Zirconate ($Li_6Zr_2O_7$), Chem. Mater., 17 (2005) 1704-1710.

[11] T. Zhao, E. Ochoa-Fernández, M. Rønning, D. Chen, Preparation and High-Temperature CO_2 Capture Properties of Nanocrystalline Na_2ZrO_3, Chem. Mater., 19 (2007) 3294-3301.

[12] L.M. Palacios-Romero, E. Lima, H. Pfeiffer, Structural Analysis and CO_2 Chemisorption Study on Nonstoichiometric Lithium Cuprates ($Li_{2+x}CuO_{2+x/2}$), J. Phys. Chem. A, 113 (2008) 193-198.

[13] Y. Zhang, Y. Gao, H. Pfeiffer, B. Louis, L. Sun, D. O'Hare, Q. Wang, Recent advances in lithium containing ceramic based sorbents for high-temperature CO_2 capture, J. Mater. Chem. A, 7 (2019) 7962-8005.

[14] X. Yan, Y. Li, X. Ma, J. Zhao, Z. Wang, Performance of Li_4SiO_4 Material for CO_2 Capture: A Review, Int. J. Mol. Sci., 20 (2019).

[15] Y. Hu, W. Liu, Y. Yang, M. Qu, H. Li, CO_2 capture by Li_4SiO_4 sorbents and their applications: Current developments and new trends, Chem. Eng. J., 359 (2019) 604-625.

[16] H. Xu, W. Cheng, X. Jin, G. Wang, H. Lu, H. Wang, D. Chen, B. Fan, T. Hou, R. Zhang, Effect of the Particle Size of Quartz Powder on the Synthesis and CO_2 Absorption Properties of Li_4SiO_4 at High Temperature, Ind. Eng. Chem. Res., 52 (2013) 1886-1891.

[17] K. Kanki, H. Maki, M. Mizuhata, Carbon dioxide absorption behavior of surface-modified lithium orthosilicate/potassium carbonate prepared by ball milling, Int. J. Hydrogen Energy, 41 (2016) 18893-18899.

[18] I.C. Romero-Ibarra, J. Ortiz-Landeros, H. Pfeiffer, Microstructural and CO_2 chemisorption analyses of Li4SiO4: Effect of surface modification by the ball milling process, Thermochim. Acta, 567 (2013) 118-124.

[19] X. Yang, W. Liu, J. Sun, Y. Hu, W. Wang, H. Chen, Y. Zhang, X. Li, M. Xu, Preparation of Novel Li_4SiO_4

Sorbents with Superior Performance at Low CO_2 Concentration, ChemSusChem, 9 (2016) 1607-1613.
[20] S. Shan, S. Li, Q. Jia, L. Jiang, Y. Wang, J. Peng, Impregnation Precipitation Preparation and Kinetic Analysis of Li_4SiO_4-Based Sorbents with Fast CO_2 Adsorption Rate, Ind. Eng. Chem. Res., 52 (2013) 6941-6945.
[21] M.J. Venegas, E. Fregoso-Israel, R. Escamilla, H. Pfeiffer, Kinetic and Reaction Mechanism of CO_2 Sorption on Li_4SiO_4:Study of the Particle Size Effect, Ind. Eng. Chem. Res., 46 (2007) 2407-2412.
[22] E. Carella, M.T. Hernandez, High lithium content silicates: A comparative study between four routes of synthesis, Ceram. Int., 40 (2014) 9499-9508.
[23] K. Wang, X. Wang, P. Zhao, X. Guo, High-Temperature Capture of CO_2 on Lithium-Based Sorbents Prepared by a Water-Based Sol-Gel Technique, Chem. Eng. Technol., 37 (2014) 1552-1558.
[24] M.R. Quddus, M.B.I. Chowdhury, H.I. de Lasa, Non-isothermal kinetic study of CO_2 sorption and desorption using a fluidizable Li_4SiO_4, Chem. Eng. J., 260 (2015) 347-356.
[25] P.V. Subha, B.N. Nair, P. Hareesh, A.P. Mohamed, T. Yamaguchi, K.G.K. Warrier, U.S. Hareesh, Enhanced CO_2 absorption kinetics in lithium silicate platelets synthesized by a sol-gel approach, J. Mater. Chem. A, 2 (2014) 12792-12798.
[26] K. Wang, Z. Zhou, P. Zhao, Z. Yin, Z. Su, J. Sun, Synthesis of a highly efficient Li4SiO4 ceramic modified with a gluconic acid-based carbon coating for high-temperature CO_2 capture, Appl. Energy, 183 (2016) 1418-1427.
[27] K. Wang, Z. Yin, P. Zhao, Synthesis of macroporous Li_4SiO_4 via a citric acid-based sol–gel route coupled with carbon coating and its CO_2 chemisorption properties, Ceram. Int., 42 (2016) 2990-2999.
[28] S. Jeoung, J.H. Lee, H.Y. Kim, H.R. Moon, Effects of porous carbon additives on the CO_2 absorption performance of lithium orthosilicate, Thermochim. Acta, 637 (2016) 31-37.
[29] K. Wang, W. Li, Z. Yin, Z. Zhou, P. Zhao, High-Capacity Li_4SiO_4-Based CO_2 Sorbents via a Facile Hydration–NaCl Doping Technique, Energy Fuels, 31 (2017) 6257-6265.
[30] M. Seggiani, M. Puccini, S. Vitolo, High-temperature and low concentration CO_2 sorption on Li_4SiO_4 based sorbents: Study of the used silica and doping method effects, Int. J. Greenhouse Gas Control, 5 (2011) 741-748.
[31] H.A. Lara-García, O. Ovalle-Encinia, J. Ortiz-Landeros, E. Lima, H. Pfeiffer, Synthesis of $Li_{4+x}Si_{1-x}Fe_xO_4$ solid solution by dry ball milling and its highly efficient CO_2 chemisorption in a wide temperature range and low CO_2 concentrations, J. Mater. Chem. A, 7 (2019) 4153-4164.
[32] P.V. Subha, B.N. Nair, V. Visakh, C.R. Sreerenjini, A.P. Mohamed, K.G.K. Warrier, T. Yamaguchi, U.S. Hareesh, Germanium-incorporated lithium silicate composites as highly efficient low-temperature sorbents for CO2 capture, J. Mater. Chem. A, 6 (2018) 7913-7921.
[33] V.L. Meja-Trejo, E. Fregoso-Israel, H. Pfeiffer, Textural, Structural, and CO_2 Chemisorption Effects Produced on the Lithium Orthosilicate by Its Doping with Sodium ($Li_{4-x}Na_xSiO_4$), Chem. Mater., 20 (2008) 7171-7176.
[34] Z.Y. Zhou, K. Wang, Z.G. Yin, P.F. Zhao, Z. Su, J. Sun, Molten K_2CO_3-promoted high-performance Li_4SiO_4 sorbents at low CO_2 concentrations, Thermochim. Acta, 655 (2017) 284-291.
[35] Q. Zhang, C. Shen, S. Zhang, Y. Wu, Steam methane reforming reaction enhanced by a novel K_2CO_3-Doped Li_4SiO_4 sorbent: Investigations on the sorbent and catalyst coupling behaviors and sorbent regeneration strategy, Int. J. Hydrogen Energy, 41 (2016) 4831-4842.
[36] M. Seggiani, M. Puccini, S. Vitolo, Alkali promoted lithium orthosilicate for CO_2 capture at high temperature and low concentration, Int. J. Greenhouse Gas Control, 17 (2013) 25-31.
[37] X. Yang, W. Liu, J. Sun, Y. Hu, W. Wang, H. Chen, Y. Zhang, X. Li, M. Xu, Alkali-Doped Lithium Orthosilicate Sorbents for Carbon Dioxide Capture, Chemsuschem, 9 (2016) 2480-2487.
[38] M. Xiang, Y. Zhang, M. Hong, S. Liu, Y. Zhang, H. Liu, C. Gu, CO_2 absorption properties of Ti- and Na-doped

porous Li_4SiO_4 prepared by a sol-gel process, J. Mater. Sci., 50 (2015) 4698-4706.

[39] P.V. Subha, B.N. Nair, A.P. Mohamed, G.M. Anilkumar, K.G.K. Warrier, T. Yamaguchi, U.S. Hareesh, Morphologically and compositionally tuned lithium silicate nanorods as high-performance carbon dioxide sorbents, J. Mater. Chem. A, 4 (2016) 16928-16935.

[40] K. Wang, Z.Y. Zhou, P.F. Zhao, Z.G. Yin, Z. Su, J. Sun, Molten sodium-fluoride-promoted high-performance Li_4SiO_4-based CO_2 sorbents at low CO_2 concentrations, Appl. Energy, 204 (2017) 403-412.

[41] K. Wang, W. Li, Z.G. Yin, Z.Y. Zhou, P.F. Zhao, High-Capacity Li_4SiO_4-Based CO_2 Sorbents via a Facile Hydration-NaCl Doping Technique, Energy Fuels, 31 (2017) 6257-6265.

[42] Y. Hu, W. Liu, Y. Yang, X. Tong, Q. Chen, Z. Zhou, Synthesis of highly efficient, structurally improved Li_4SiO_4 sorbents for high-temperature CO_2 capture, Ceram. Int., 44 (2018) 16668-16677.

[43] S. Singh, A.K. Raj, R. Sen, P. Johari, S. Mitra, Impact of Cl Doping on Electrochemical Performance in Orthosilicate (Li_2FeSiO_4): A Density Functional Theory Supported Experimental Approach, ACS Appl. Mat. Interfaces, 9 (2017) 26885-26896.

[44] B. Philippe, R. Dedryvère, J. Allouche, F. Lindgren, M. Gorgoi, H. Rensmo, D. Gonbeau, K. Edström, Nanosilicon Electrodes for Lithium-Ion Batteries: Interfacial Mechanisms Studied by Hard and Soft X-ray Photoelectron Spectroscopy, Chem. Mater., 24 (2012) 1107-1115.

[45] B. Philippe, R. Dedryvere, M. Gorgoi, H. Rensmo, D. Gonbeau, K. Edstrom, Role of the $LiPF_6$ Salt for the Long-Term Stability of Silicon Electrodes in Li-Ion Batteries - A Photoelectron Spectroscopy Study, Chem. Mater., 25 (2013) 394-404.

[46] H.W. Nesbitt, G.M. Bancroft, G.S. Henderson, R. Ho, K.N. Dalby, Y. Huang, Z. Yan, Bridging, non-bridging and free (O^{2-}) oxygen in Na_2O-SiO_2 glasses: An X-ray Photoelectron Spectroscopic (XPS) and Nuclear Magnetic Resonance (NMR) study, J. Non-Cryst. Solids, 357 (2011) 170-180.

[47] A. Sharma, H. Jain, A.C. Miller, Surface Modification of a Silicate Glass during XPS Experiments, Surface & Interface Analysis, 31 (2001) 369-374.

[48] J. Lu, M. Luo, C. Li, TPR and XPS studies of NaCl modified $VCe_{0.2}Cu_{0.8}$ catalysts for direct propylene epoxidation, Reaction Kinetics & Catalysis Letters, 86 (2005) 219-224.

[49] B. González, J. Blamey, M.J. Al-Jeboori, N.H. Florin, P.T. Clough, P.S. Fennell, Additive effects of steam addition and HBr doping for CaO-based sorbents for CO_2 capture, Chem. Eng. Process., 103 (2016) 21-26.

[50] M. Niu, X. Li, J. Ouyang, H. Yang, Lithium orthosilicate with halloysite as silicon source for high temperature CO_2 capture, Rsc Advances, 6 (2016) 44106-44112.

[51] J.i. Ida, Y.S. Lin, Mechanism of High-Temperature CO_2 Sorption on Lithium Zirconate, Environ. Sci. Technol., 37 (2003) 1999-2004.

[52] Q. Zhang, D.Y. Han, Y. Liu, Q. Ye, Z.B. Zhu, Analysis of CO_2 Sorption/Desorption Kinetic Behaviors and Reaction Mechanisms on Li_4SiO_4, AlChE J., 59 (2013) 901-911.

[53] K. Wang, J. Hong, Z. Zhou, Z. Lin, P. Zhao, Development of Alkali Nitrate-Containing Li_4SiO_4 for High-Temperature CO_2 Capture, Energy Technology, 7 (2019) 325-332.

[54] K. Wang, C. Wang, Z. Zhou, Z. Lin, P. Zhao, Synthesis of LiF-Containing Li_4SiO_4 as Highly Efficient CO_2 Sorbents, Ind. Eng. Chem. Res., 57 (2018) 8085-8092.

Tables

Table 1. N_2 adsorption results of three samples

Samples	Surface area (m^2/g)	Pore volume (cm^3/g)	Pore diameter (nm)
SCT	0.78	0.81×10^{-3}	2.19
SCT-NaBr-0.1	1.27	2.23×10^{-3}	1.22
SCT-NaCl-0.1	0.42	0.67×10^{-3}	2.55

Table 2. Kinetic parameters obtained from the isotherms of the samples

Samples	t [°C]	k_1 [s^{-1}]	k_2 [s^{-1}]	A	B	C	R
SCT	475	5.71×10^{-2}	1.39×10^{-3}	-5.33	-38.45	144.56	0.998
	525	1.77×10^{-1}	1.95×10^{-2}	-3.75	-12.41	116.70	0.999
	575	2.01×10^{-2}	3.45×10^{-2}	-12.21	-15.48	123.48	0.990
SCT-NaCl-0.1	475	6.06×10^{-2}	4.57×10^{-3}	-14.10	-21.94	138.04	0.997
	525	3.08×10^{-1}	2.28×10^{-2}	-16.32	-13.75	129.83	0.997
	575	9.88×10^{-1}	2.08×10^{-1}	14.52	-46.16	133.13	0.989
SCT-NaBr-0.1	475	1.32×10^{-1}	9.14×10^{-3}	-19.04	-11.57	131.85	0.997
	525	3.73×10^{-1}	3.59×10^{-2}	-25.11	-6.64	128.91	0.995
	575	8.49×10^{-1}	1.98×10^{-1}	13.63	-43.79	131.25	0.997

Figures

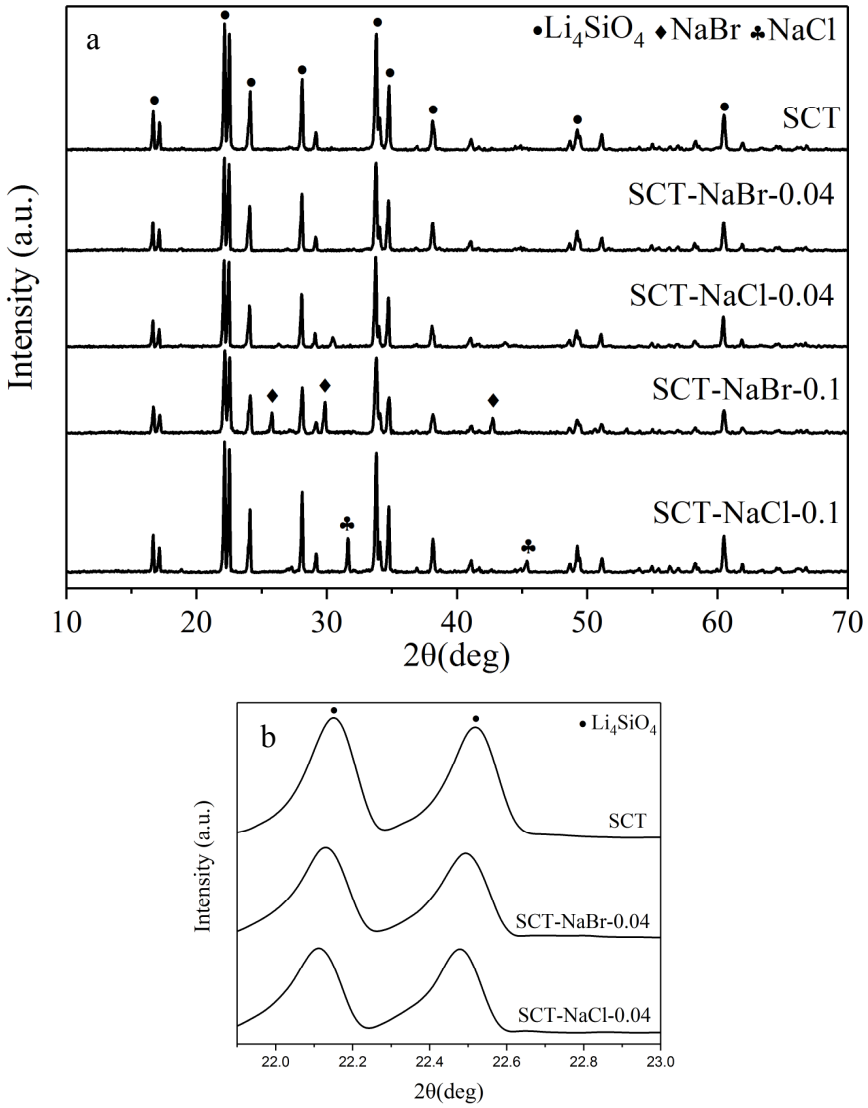

Fig. 1.

Fig. 1. XRD patterns of samples. (a) 2θ range from 10° to 70°; (b) 2θ range from 21.8° to 23.0°.

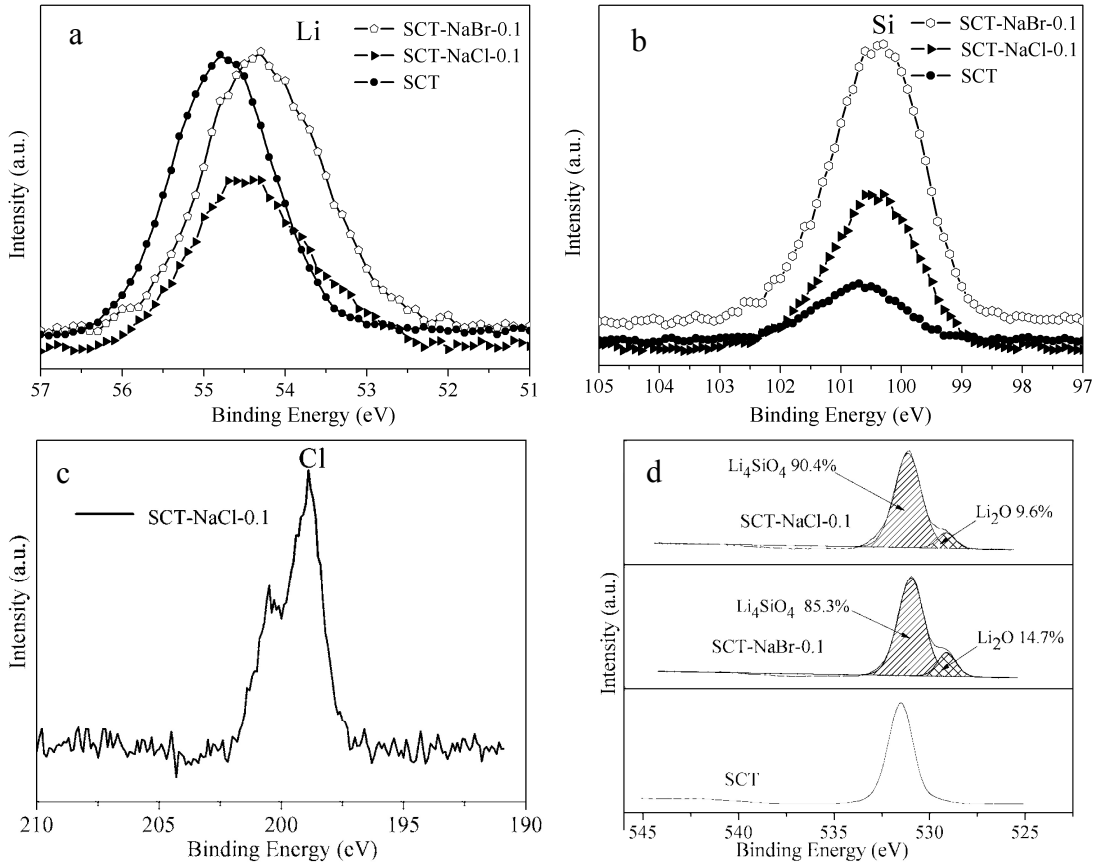

Fig. 2.

Fig. 2. XPS spectra of samples. (a) Li 1s spectra; (b) Si 2p spectra; (c) Cl 2p spectra; (b) O 1s spectra.

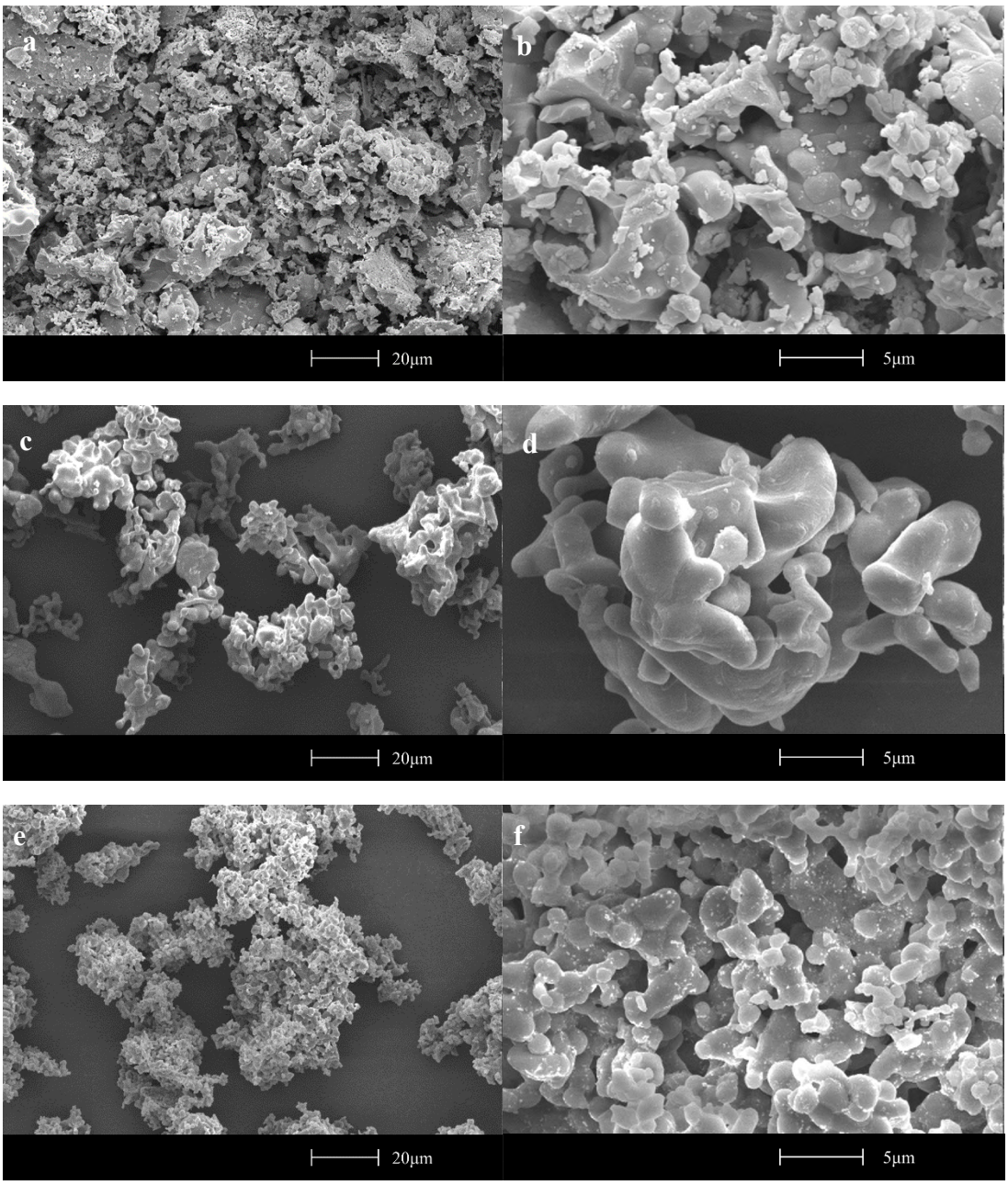

Fig. 3.

Fig. 3. SEM images of different samples: (a, b) SCT; (c, d) SCT-NaCl-0.1; (e, f) SCT-NaBr-0.1.

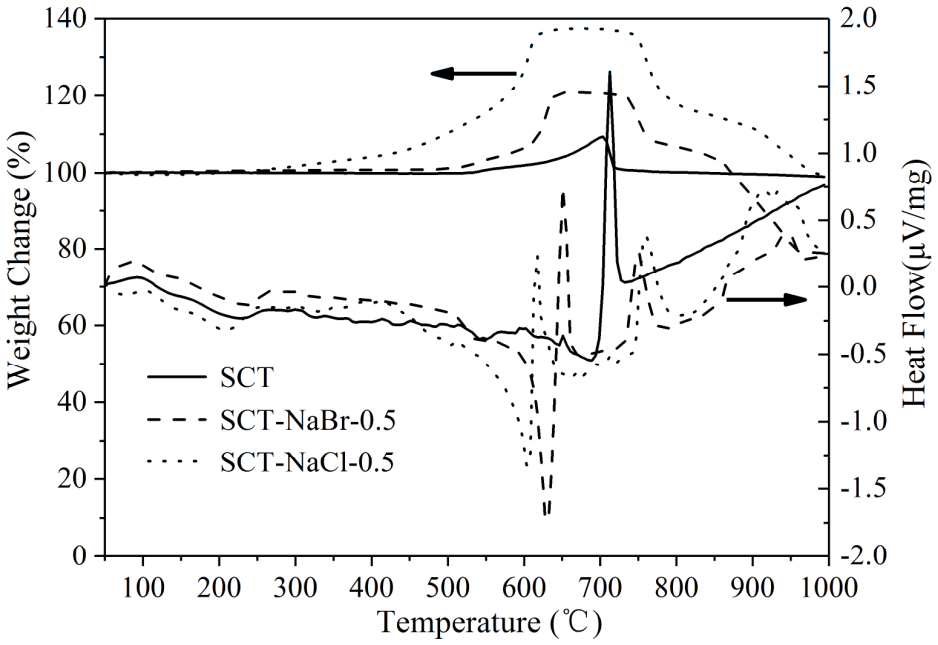

Fig. 4.

Fig. 4. CO_2 uptake characteristics of samples with dynamic thermogravimetric curves between 20 and 1000 °C in a 100% CO_2 flux.

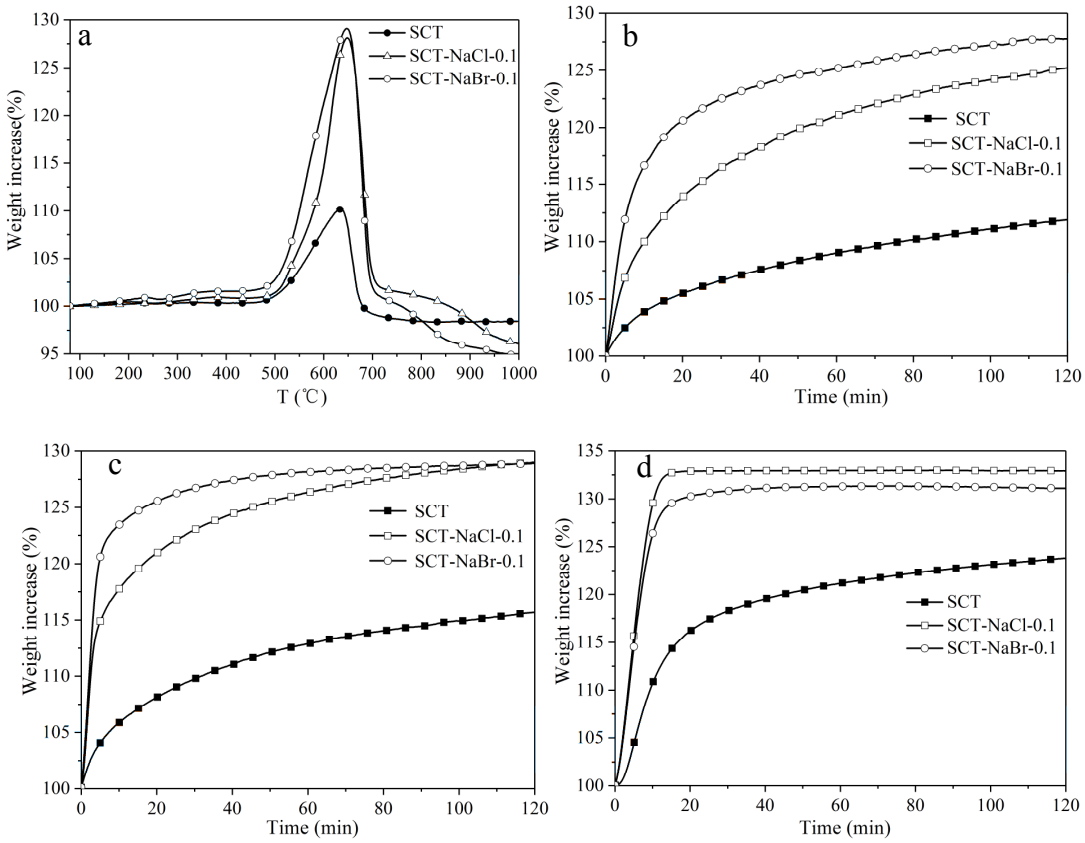

Fig. 5.

Fig. 5. CO_2 uptake characteristics of three samples in a 15% CO_2 flux. (a) Dynamic thermogravimetric curves between 80 and 1000 °C. (b) Isothermal curves at 475 °C; (c) Isothermal curves at 525 °C. (d) Isothermal curves at 575 °C.

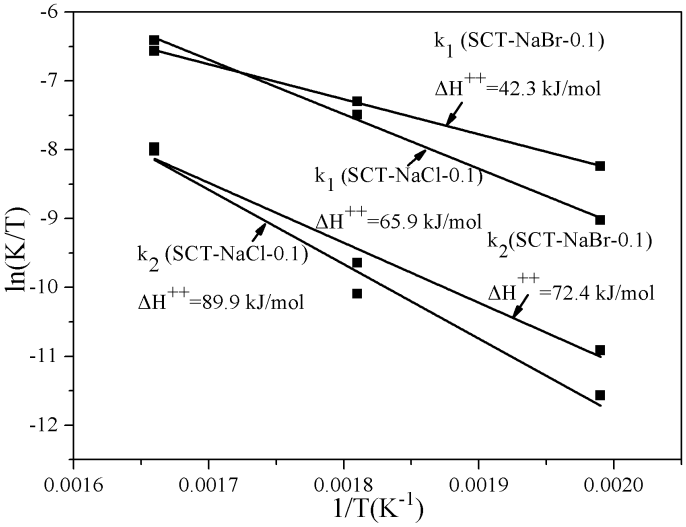

Fig. 6.

Fig. 6. Eyring's plots for the rate constants of the surface chemisorption (k_1) and lithium diffusion (k_2) of SCT-NaCl-0.1and SCT-NaBr-0.1.

Supplementary material

Manuscript title: **Sorption of CO_2 on NaBr co-doped Li_4SiO_4 ceramics: Structural and kinetic analysis**

Ke Wang[1,2], Youwei Zhao[1], Peter T. Clough[2], Pengfei Zhao[1], Edward J. Anthony[2*]

[1] School of Electrical and Power Engineering, China University of Mining and Technology, Xuzhou 221116, China.

[2] Energy and Power Theme, Cranfield University, Cranfield, Bedfordshire, MK43 0AL, UK.

Ke Wang is currently a visiting professor at Cranfield University.

* Corresponding author: Edward J. Anthony, E: b.j.anthony@cranfield.ac.uk, T: +44 (0) 1234 752 823

Figure caption:

Fig. S1. The dynamic DSC curves between 20 and 750 °C in a 100% CO_2 flux for three sorbents.

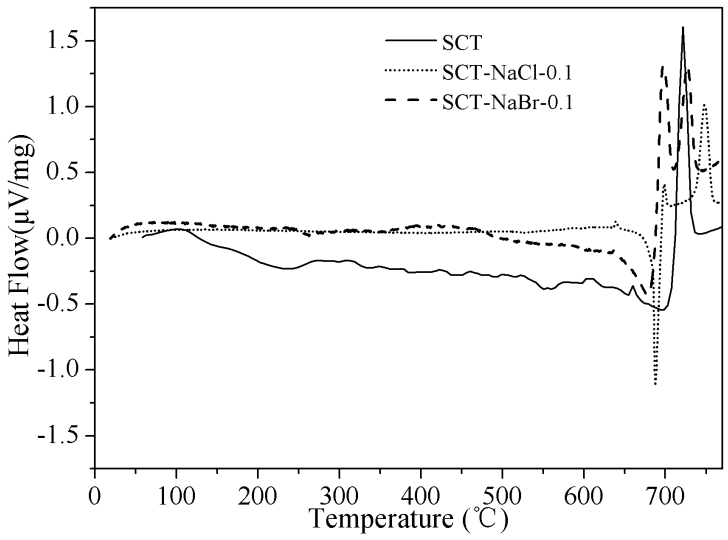

Fig. S1.

Sorption of CO2 on NaBr co-doped Li4SiO4 ceramics: Structural and kinetic analysis

Wang, Ke

2019-07-13

Wang K, Zhao Y, Clough PT, et al., Sorption of CO2 on NaBr co-doped Li4SiO4 ceramics: Structural and kinetic analysis. Fuel Processing Technology, Volume 195, December 2019, Article number 106143

https://doi.org/10.1016/j.fuproc.2019.106143